

Magnesium isotope fractionation in silicate melts by chemical and thermal diffusion

Frank M. Richter^{a,*}, E. Bruce Watson^b, Ruslan A. Mendybaev^a,
Fang-Zhen Teng^a, Philip E. Janney^c

^a Department of the Geophysical Sciences, The University of Chicago, 5734 South Ellis Avenue, Chicago, IL 60637, USA

^b Department of Earth & Environmental Sciences, Rensselaer Polytechnic Institute, Troy, NY 12180, USA

^c Arizona State University, School of Earth and Space Exploration, P.O. Box 871404, Tempe, AZ 85287, USA

Received 31 May 2007; accepted in revised form 16 October 2007; available online 30 October 2007

Abstract

Two types of laboratory experiments were used to quantify magnesium isotopic fractionations associated with chemical and thermal (Soret) diffusion in silicate liquids. Chemical diffusion couples juxtaposing a molten natural basalt (SUNY MORB) and a molten natural rhyolite (Lake County Obsidian) were run in a piston cylinder apparatus and used to determine the isotopic fractionation of magnesium as it diffused from molten basalt to molten rhyolite. The thermal diffusion experiments were also run in a piston cylinder apparatus but with a sample made entirely of molten SUNY MORB displaced from the hotspot of the assembly furnace so that the sample would have a temperature difference of about 100–200 °C from one end to the other. The chemical diffusion experiments showed fractionations of $^{26}\text{Mg}/^{24}\text{Mg}$ by as much as 7‰, which resulted in an estimate for the mass dependence of the self-diffusion coefficients of the magnesium isotopes corresponding to $D_{^{26}\text{Mg}}/D_{^{24}\text{Mg}} = (24/26)^\beta$ with $\beta = 0.05$. The thermal diffusion experiments showed that a temperature difference of about 100 °C resulted in the MgO, CaO, and FeO components of the basalt becoming slightly enriched by about 1 wt% in the colder end while SiO₂ was enriched by several wt% in the hotter end. The temperature gradient also fractionated the magnesium isotopes. A temperature difference of about 150 °C produced an 8‰ enrichment of $^{26}\text{Mg}/^{24}\text{Mg}$ at the colder end relative to the hotter end. The magnesium isotopic fractionation as a function of temperature in molten basalt corresponds to $3.6 \times 10^{-2}\text{‰}/^\circ\text{C}/\text{amu}$.

© 2007 Elsevier Ltd. All rights reserved.

1. INTRODUCTION

The work reported here began as a relatively straightforward extension to magnesium of our earlier work on the kinetic isotope fractionation of calcium and lithium during chemical diffusion between molten basalt and rhyolite. In Richter et al. (2003) we reported on laboratory experiments showing large isotopic fractionations of calcium (~6‰ for $^{44}\text{Ca}/^{40}\text{Ca}$) and lithium (~40‰ for $^7\text{Li}/^6\text{Li}$) as they diffused

from molten basalt to molten rhyolite. Based on the isotopic fractionation we had observed for calcium we predicted that chemical diffusion could lead to fractionations of $^{26}\text{Mg}/^{24}\text{Mg}$ by as much as 10‰ given a sufficient, and not unreasonable, difference in the magnesium concentration between basalt and rhyolite (see Fig. 9 in Richter et al., 2003). In terms of potential applications of kinetic isotope fractionations by diffusion to petrology, the best chemical elements will be those that have sufficiently abundant stable isotopes for high-precision isotopic measurements, sufficiently large differences in the parent element concentration between naturally occurring igneous rock types, and very little difference in the isotopic composition of the igneous rocks. The last of these attributes insures that attempts to

* Corresponding author.

E-mail address: richter@geosci.uchicago.edu (F.M. Richter).

identify kinetic isotope fractionations are not compromised by effects due to mixing materials of different isotopic composition. Of the major rock forming elements, magnesium fits these requirements best.

As in our earlier work, rhyolite–basalt diffusion couples were run in a piston cylinder apparatus at pressures of about 15 kbars and temperatures of about 1400 °C. Our initial efforts to determine the isotopic fractionation associated with the transport of magnesium from the molten basalt with about 9 wt% MgO into the rhyolite with negligible magnesium showed, as we expected, that the magnesium that diffused was isotopically light by about 7‰ in $^{26}\text{Mg}/^{24}\text{Mg}$. However, when we tried to simultaneously model the magnesium elemental and isotopic profiles we ran into problems. Most obviously, we were not able to account for a large systematic gradient in the magnesium isotopic composition in the basalt part of the couple. This isotopic gradient in the basalt was both much larger than the analytical precision of the measurements and opposite in sign from what we calculated for kinetic fractionation. We had seen a similar effect before in one of the rhyolite–basalt diffusion couples that were used to determine the diffusive isotopic fractionation of calcium (sample RB2, Fig. 6 of Richter et al., 2003). At that time we had no explanation for the calcium isotopic gradient in the basalt side of RB2, and so decided to redo the experiment by making a second similar diffusion couple (RB3 in Richter et al., 2003). The calcium isotopic data from this second couple did not show a significant isotopic gradient in the basalt. Both RB2 and RB3 showed similarly fractionated calcium isotopes in the rhyolite part of the couple and we used this to infer the relative mobility of calcium isotopes in the silicate melt. The issue of how to explain the calcium isotopic gradient in the basalt side of RB2 was left unresolved.

Our finding, once again, a significant isotopic gradient in the basalt side of a rhyolite–basalt diffusion couple that we could not explain by the relative mobility of the isotopes as they diffused from the basalt made the issue hard to ignore. We now believe that the cause for this was a thermal gradient in the piston cylinder assembly containing the molten sample. Kyser et al. (1998) had already shown that thermal gradients of about 50 °C/mm across a silicate liquid could fractionate oxygen isotopes by several per mil. In order to explain the magnitude of the magnesium isotopic fractionation in the basalt shown in Fig. 4 as being due to a thermal gradient would require that a temperature change of several tens of degree centigrade across a 10 mm diffusion couple produce magnesium isotopic fractionations of several per mil per atomic mass unit. A temperature difference of several tens of degree centigrade over 10 mm is quite possible in a standard piston cylinder experiment (see Figs. 1 and 2) unless special efforts are taken to enlarge the hotspot by using tapered heaters and carefully centering relatively small assemblies (5 mm rather than 10 mm) in the hotspot. The obvious thing to do was to carry out experiments to determine whether temperature gradients across molten basalt can give rise to the large magnesium isotopic fractionations required by our proposed explanation for the magnesium isotopic data in the basalt part of sample

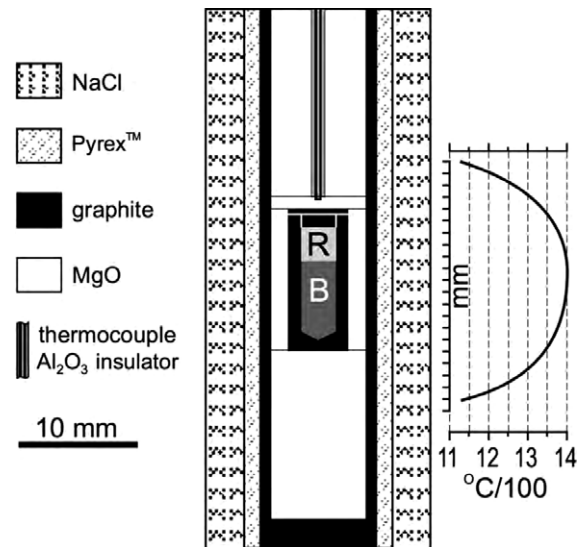


Fig. 1. Schematic diagram of the piston cylinder assembly used for the rhyolite–basalt diffusion experiments and for the thermal diffusion (i.e., Soret diffusion) experiments in which case the starting material was entirely basalt. Also shown is the temperature profile along the axis of the assembly as determined by Watson et al. (2002) for this assembly at 1400 °C and 1.0 GPa.

RB11. What we found were magnesium isotopic fractionations in molten basalt of about 8‰ in $^{26}\text{Mg}/^{24}\text{Mg}$ for a temperature difference of not much more than 100 °C. Having identified the likely source of the isotopic fractionation of magnesium isotopes in the basalt side of our rhyolite–basalt diffusion couples, we modified the rhyolite–basalt experiments by using smaller sample containers to minimize temperature differences in order that the measured isotopic fractionations would reflect only the relative mobility of the isotopes during chemical diffusion. The relative mobility of the magnesium isotopes resulted in kinetic fractionations of about 7‰ in $^{26}\text{Mg}/^{24}\text{Mg}$ as magnesium diffused from basalt into rhyolite. We also carried out a series of longer duration thermal diffusion experiments to determine whether the magnesium isotopic fractionations would persist as the system approached a steady state. The longer duration runs showing that the isotopic fractionations had persisted were used to determine a relationship between temperature differences across molten basalt and the associated magnesium isotopic fractionation. Details regarding the chemical and thermal diffusion experiments are given in Table 1.

2. EXPERIMENTAL AND ANALYTICAL METHODS

The diffusion couples used in the present study were made by juxtaposing molten natural basalt (SUNY MORB) and molten natural rhyolite (Lake County Obsidian) in graphite capsules run in a piston cylinder apparatus. The thermal diffusion experiments were run in the same way except that the starting material was entirely SUNY MORB. The composition of the starting materials is given

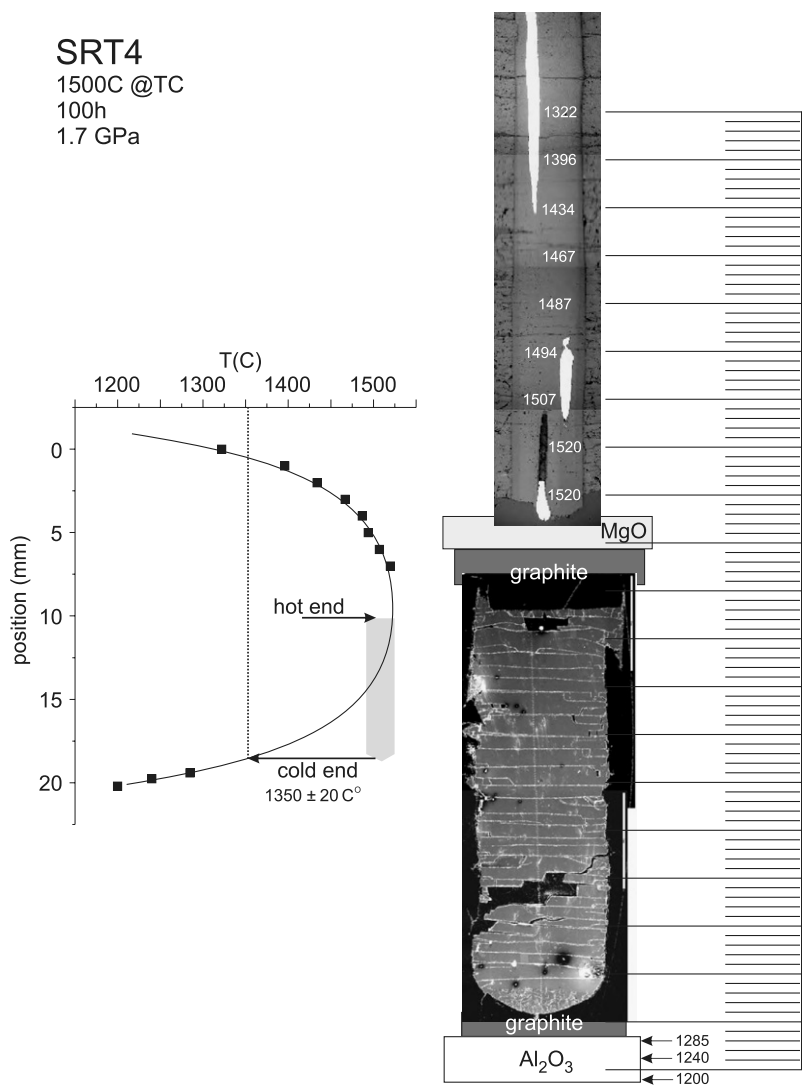


Fig. 2. The picture on the right shows a backscattered electron image of the exposed portion of quenched glass enclosed in graphite recovered from SRT4, a thermal diffusion experiment with basalt as the starting material. Decompression fractures can be seen as light colored lines. At the very bottom end of the sample one can see a small region ($\sim 400 \mu\text{m}$) where a small amount of olivine crystallized. The scale bar on the right is in mm further subdivided into 200 μm intervals. In the upper part of the picture we show a ground-down portion of the alumina (Al_2O_3) tube used to isolate thermocouple wires, which show up as white where exposed. The alumina tube was surrounded by MgO and the temperatures indicated at various points along the alumina tube were determined by the thickness of the spinel layer that formed during the run by the reaction of Al_2O_3 with MgO (see [Watson et al., 2002](#) for a description of the spinel thermometry method). MgO chips were also placed in contact with the alumina spacer at the bottom of the assembly allowing for a determination of temperature there. The graph on the left shows the spinel-derived temperature determinations and the location of the molten basalt sample in the temperature profile. The more complete temperature measurements reported by [Watson et al. \(2002\)](#) for this specific piston assembly was used to specify the temperature profile in the molten basalt.

Table 1
Experimental condition

Experiment	Run duration (h)	Temperature (°C)	Pressure (GPa)
RB11	15	1400	1.0
RBX	15	1400	1.2
SRT3	20	1330–1510	1.3
SRT4	100	1350–1520	1.7
SRT8	63.8	1415–1505	1.5

in Table 1 of [Richter et al. \(2003\)](#). Fig. 1 shows a schematic diagram of the piston cylinder assembly along with a typical temperature profile in the assembly. All the experiments reported here were run at pressures between 1.0 and 1.7 GPa (see Table 1) in order to take advantage of the temperature gradients inherent in the piston cylinder assemblies, while at the same time avoiding complications due to bubble formation that can plague experiments at near-atmospheric pressure. We used pressures at or above 1 GPa because piston cylinder runs are more stable at high-

er pressures. A small amount of air may have been trapped during pressurization of the starting powders. This would amount at most to a few hundred parts per million dissolved N₂ and an even smaller amount of trapped oxygen that probably converted to dissolved CO₂ by reaction with the graphite container. These volatiles will have had a negligible effect on the bulk properties of the melt.

An important part of the present study involves thermal diffusion and thus it is important that we be able to determine the thermal gradients in our experiments. For this purpose, we used a method recently developed by Watson et al. (2002) based on the kinetics of the spinel-forming reaction $\text{MgO} + \text{Al}_2\text{O}_3 \rightarrow \text{MgAl}_2\text{O}_4$. Piston cylinder assemblies use the refractory oxides MgO and Al₂O₃ as insulators and filler materials, and thus there is ample opportunity to juxtapose these in various parts of the assembly to form spinel. Watson et al. (2002) calibrated the rate at which spinel is formed as a function of both pressure and temperature in various types of piston cylinder assemblies including the one used here, and thus given the duration of an experiment, the pressure, and the thickness of the spinel layer that formed, the temperature at each point where MgO and Al₂O₃ were in contact can be determined with a precision of about ± 20 °C. Fig. 2 shows the temperatures measured by the spinel-reaction thermometer above and below the sample in one of our experiments. The temperature profile within the molten sample was not measured but the shape of this profile can be inferred from the more complete thermal structure measured by Watson et al. (2002) for the same piston cylinder assembly that we used for the experiments reported here.

The chemical and thermal diffusion couples recovered from the piston cylinder runs were polished to expose the quenched glass and then the major element concentrations were measured using a JOEL JSM-5800LV scanning electron microscope equipped with an Oxford Link ISIS-300 energy dispersive X-ray microanalysis system. The concentration of each analyzed spot was derived by rastering the beam over a 10 μm^2 area. The analysis conditions involved a 15 kV primary beam current of 8 nA, which gives a typical precision of better than 1% relative. Two or more major element profiles were measured for each couple. The chemical composition of the experimental samples was found to be uniform along profiles perpendicular to the long axis of the sample.

After the major element profiles had been measured the samples were cut perpendicular to their long axis to make a series of approximately 500 μm thick slabs. These slabs were dissolved overnight in a 70 °C 3:1 mixture of HF/HNO₃. The dissolved samples were converted to 1 N nitric acid solutions by evaporating and redissolving them two times in high-purity, double distilled concentrated nitric acid followed by a final dry down by evaporation and redissolution in 1 N nitric acid. One hundred microliters of the 1 N nitric acid sample solution containing between 0.5 and 5 μg of Mg was put through an ion exchange column holding approximately 1 ml of AG50W-X8 resin (200–400 mesh) in order to separate the magnesium. All samples in this study were put through the ion exchange column twice to insure that the Al/Mg and Ca/Mg ratios were sufficiently small (i.e., below 0.02) that matrix effects would be negli-

ble (Galy et al., 2001). The final step in preparing the magnesium for isotopic analysis was to dry down and redissolve a fraction of the purified magnesium in 3 wt% high-purity nitric acid to make a solution with 200 ppb magnesium.

The magnesium isotopic compositions of the starting material (SUNY MORB) and the sections taken from the chemical and thermal diffusion couples were measured using the Micromass Isoprobe multi-collector inductively coupled plasma mass spectrometer in the Isotope Geochemistry Laboratory at the Field Museum in Chicago Illinois. A CETAC Aridus desolvating nebulizer was used to introduce sample solution into the mass spectrometer. The three isotopes of magnesium (²⁴Mg, ²⁵Mg, ²⁶Mg) and ²⁷Al were measured simultaneously by static multi-collection using four Faraday collectors (L3, axial, H4 and H6). Each measurement consisted of a 60 s “on-peak” blank measurement followed by 20 10 s cycles of sample measurement. Each sample analysis is bracketed by measurements of the DSM3 standard (Galy et al., 2003) to correct for instrumental isotope fractionation. During the course of an analytical session each unknown was analyzed at least four times, and at least one other basalt standard (either BCR-2 or SUNY MORB) was also analyzed. With an uptake rate of 100 ml/min a 200 ppb solution typically produced ion currents of $3.5\text{--}4 \times 10^{-11}$ A for ²⁴Mg. The in-run precision of the ²⁶Mg/²⁴Mg measurements is $< \pm 0.02\%$ (2SD), while the external precision based on duplicate runs of SUNY MORB during the course of these measurements (December 2006 to March 2007) is $\pm 0.1\%$ (2SD). The measured magnesium isotopic composition of the various samples is given in Table 2.

3. CHEMICAL DIFFUSION

The main objective of the chemical diffusion experiments was to determine the mass-dependent isotopic fractionation of magnesium as it diffused from the basalt into the rhyolite. Fig. 3 shows concentration profiles for major elements in rhyolite–basalt diffusion couple RB11 run for 15 h at 1400 °C. The profiles are very similar to those reported in Richter et al. (2003), including the obvious uphill diffusion of the Al₂O₃ component. Also shown in Fig. 3 is the measured ²⁶Mg/²⁴Mg in per mil for 0.5 mm thick sections at various places along the diffusion couple. Model calculations were used to find parameters for fitting the elemental profiles and the isotopic data. The calculations are based on a one-dimensional conservation equation

$$\frac{\partial \rho_i}{\partial t} = \frac{\partial}{\partial x} \left(D_i \frac{\partial \rho_i}{\partial x} \right) \quad (1)$$

where ρ_i is the molar density (mol/cm^3) of element or isotope i and D_i is a chemical diffusion coefficient that is allowed to be a function of the local SiO₂ content of the melt to the degree needed to fit the diffusion profiles. As was done in Richter et al. (2003), we assume an effect of SiO₂ on the diffusion coefficients of the form $D_{i(\text{SiO}_2)} = D_{i,0} e^{-\alpha(f_{\text{SiO}_2} - 0.5)}$ where f_{SiO_2} is the weight fraction of SiO₂ and α is the parameter that allows us to take into account that chemical diffusion is significantly slower the greater the SiO₂ content of the melt. The initial conditions

Table 2
Magnesium isotopic data relative to standard DSM3

Sample	Distance ^c (μm)	Temperature (°C)	δ ²⁶ Mg	2σ	δ ²⁵ Mg	2σ
MORB 3-06 ^a			−0.28	0.06	−0.14	0.06
MORB 12-06 ^b			−0.32	0.07	−0.17	0.06
SRT3-1	4751	1477	−1.09	0.06	−0.54	0.02
SRT3-2	1138	1508	−2.52	0.04	−1.29	0.06
SRT3-3	8859	1336	2.42	0.10	1.25	0.06
SRT3-4	2846	1499	−1.80	0.01	−0.90	0.03
SRT3-5	6582	1435	0.36	0.10	0.18	0.03
SRT4-2	362	1520	−3.81	0.07	−1.94	0.03
SRT4-3	942	1518	−3.51	0.05	−1.81	0.08
SRT4-5	2319	1512	−2.68	0.05	−1.36	0.03
SRT4-7	3478	1503	−1.59	0.09	−0.81	0.03
SRT4-9	4710	1488	−0.30	0.10	−0.15	0.02
SRT4-11	6086	1460	1.28	0.06	0.66	0.04
SRT4-13	7608	1410	4.80	0.06	2.45	0.03
SRT8-1	8663	1414	4.36	0.03	2.22	0.05
SRT8-2	8069	1431	2.99	0.03	1.54	0.05
SRT8-5	6289	1470	0.20	0.09	0.07	0.03
SRT8-8	3679	1498	−1.55	0.03	0.80	0.05
SRT8-10	1899	1504	−2.05	0.04	−1.05	0.04
SRT8-12	297	1505	−2.07	0.06	−1.08	0.06
RB11-Y1	10008		−0.57	0.67	−0.29	0.36
RB11-Y2	8842		−6.68	0.17	−3.42	0.01
RB11-Y3	8022		−4.24	0.24	−2.18	0.07
RB11-Y4	9141		−1.64	0.04	−0.82	0.06
RB11-Y5	6623		−1.27	0.06	−0.66	0.03
RB11-Y6	5505		−1.20	0.04	−0.61	0.03
RB11-B1	704		1.29	0.03	0.68	0.05
RB11-B2	3151		−0.66	0.05	−0.32	0.03
RB11-B3	1835		0.07	0.03	0.05	0.05
RBX-1	600		0.15	0.06	0.04	0.04
RBX-2	1565		−0.14	0.02	−0.04	0.04
RBX-3	2266		−0.56	0.05	−0.27	0.05
RBX-4	2900		−1.24	0.07	−0.62	0.03
RBX-5	3457		−7.11	0.11	−3.66	0.09
RBX-6	3841		−2.96	0.14	−1.60	0.05

^a SUNY MORB measured 39 times between March 23, 2006 and April 4, 2007.

^b SUNY MORB measured 4 times on December 4, 2006.

^c Distance to the center of section sampled.

are a step function between the rhyolite elemental composition and that of the basalt together with the assumption that the rhyolite and the basalt have the same isotopic composition. The boundary condition imposed at each end of the diffusion couple is no flux (i.e., $\partial\rho_i/\partial x = 0$). In the case of isotopes we allow for the possibility that they differ in their diffusion rate, which we parameterize as

$$\frac{D_{1,o}}{D_{2,o}} = \left(\frac{m_2}{m_1}\right)^\beta \quad (2)$$

where m_1 and m_2 are the mass of isotopes 1 and 2, and β is an empirical kinetic parameter to be determined by fitting the measured isotopic fractionations associated with the diffusive transport from basalt to rhyolite.

Fig. 4 shows our best effort to fit the MgO profile from RB11, and also the isotopic fractionation of magnesium. To first order the calculated profiles do a reasonable job fitting the data, but with some important exceptions. We

failed to reproduce the local rise of MgO between 2000 μm and end of the diffusion couple at 0 μm. We were similarly unable to fit the local changes in slope of the SiO₂ and FeO profiles between 0 and 2000 μm (see Fig. 3). There were also problems with fitting the Mg isotopic data, most notably in that the model calculations indicate a small (<0.5‰) enrichment in δ²⁶Mg in the basalt side of the couple whereas the data show a gradient in δ²⁶Mg in the basalt with a total range of about 3‰. The magnesium isotopic fractionation in the basalt part of RB11 is similar to that of Ca found by Richter et al. (2003) in diffusion couple RB2. The fact that SiO₂, MgO, and FeO concentration profiles in the region 0–2000 μm have well-resolved changes in gradient where no such changes are expected based on chemical diffusion can only mean that there is some additional effect giving rise to a flux of these components. The fact that the local changes in the SiO₂ and MgO gradients are opposite (i.e., SiO₂ decreasing while MgO is increasing)

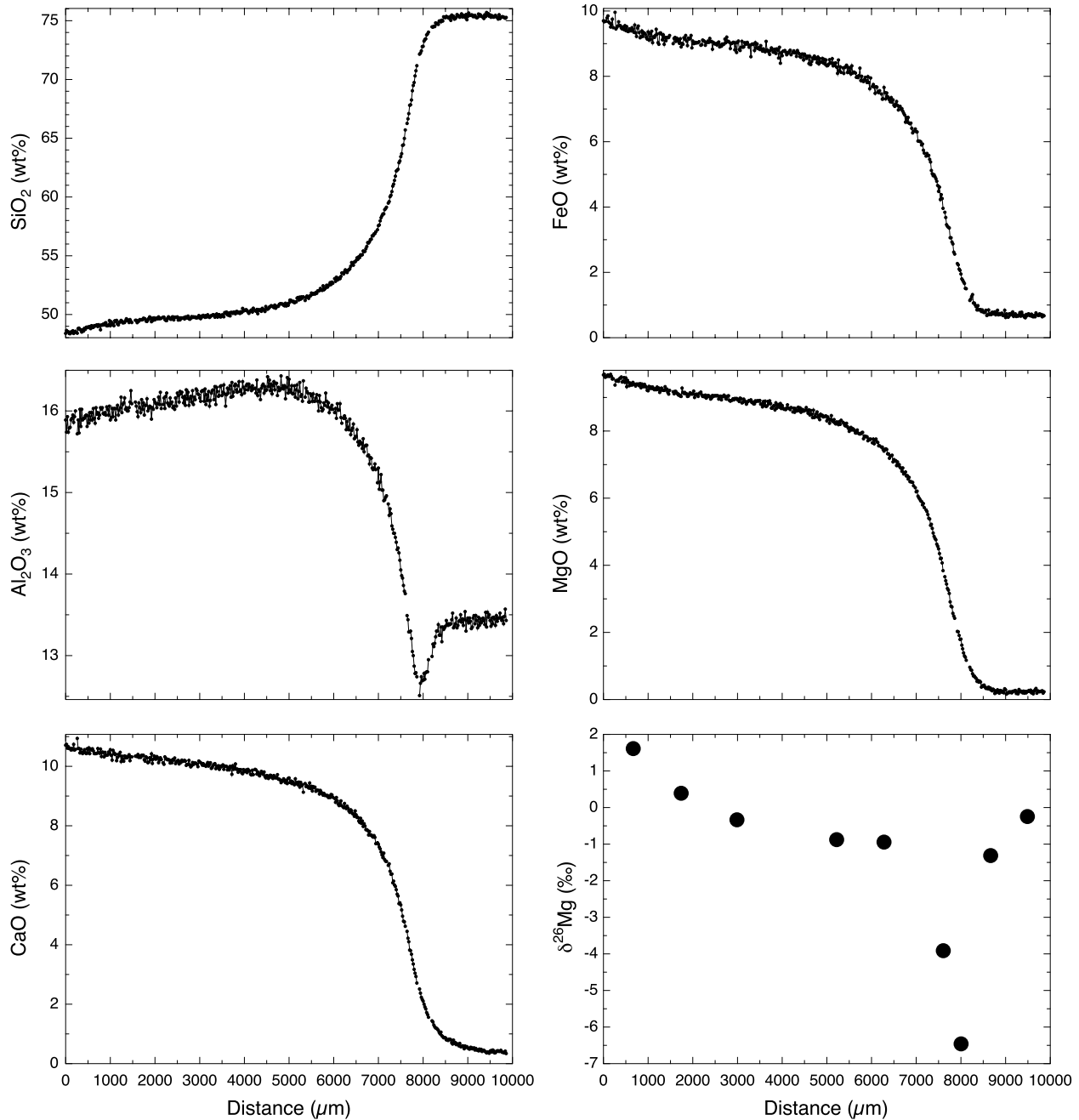


Fig. 3. Major element profiles in wt% from experiment RB-11 (15.0 h at 1400 °C) measured by energy dispersive X-ray microanalyses. These profiles are very typical of the interdiffusion of rhyolite and basalt (see Richter et al., 1999). The local minimum at on the Al₂O₃ profile is due to uphill diffusion and the asymmetry of the other elemental profiles is the result of faster diffusion in the basalt compared to in the rhyolite. The panel on the lower right shows the magnesium isotopic composition at selected points in terms of $\delta^{26}\text{Mg} \equiv 1000 \left(\frac{{}^{26}\text{Mg}/{}^{24}\text{Mg}_{\text{sample}}}{{}^{26}\text{Mg}/{}^{24}\text{Mg}_{\text{standard}}} - 1 \right)$. The standard used is DSM3 (Galy et al., 2003).

pointed to the source of the additional flux being a temperature gradient. The anti-correlation of gradients in MgO, CaO, FeO with that of SiO₂ is typical of thermal diffusion separations in silicate liquids as was shown in a series of experiments by Walker et al. (1981), Walker and DeLong (1982), and Leshner and Walker (1986). These experiments showed that when an initially isochemical melt is placed in a temperature gradient the cold end becomes enriched

in MgO, CaO, FeO, and depleted in SiO₂. If one looks carefully at the left end of the profiles shown in Fig. 3, this is exactly what one sees, which we take as evidence that experiment RB11 was affected by an unintended temperature gradient. However, for a temperature gradient to also explain the Mg isotopic gradient in the basalt we would have to show that a temperature difference sufficient to change the MgO composition by only about 1 wt% will also frac-

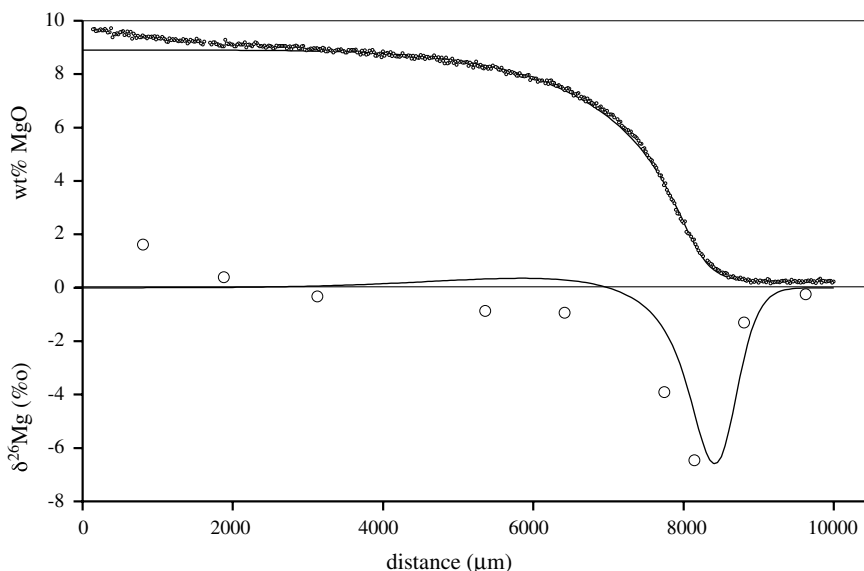


Fig. 4. The magnesium data from Fig. 3 is shown here together with calculated diffusion profiles for both the wt% MgO and the associated magnesium isotopic fractionation. The only parameter used for fitting the wt% MgO profile is the dependence of the effective binary diffusion coefficient of magnesium on the silica content of the melt. Note the misfit between the MgO data and the calculated profile at the left end. The magnesium isotopic profile was calculated using $D_{26\text{Mg}}/D_{24\text{Mg}} = (24/26)^\beta$ and $\beta = 0.05$ for the ratio of the effective diffusion coefficients of ^{26}Mg and ^{24}Mg . Given the calculated wt% MgO profile, there is no choice of $D_{26\text{Mg}}/D_{24\text{Mg}}$ that will reduce the misfit of calculated magnesium isotopic fractionations. The greatest systematic misfit is in the basalt side of the couple where we do not reproduce the decline in $\delta^{26}\text{Mg}$ between 0 and 6500 μm . The 2σ error bars for $\delta^{26}\text{Mg}$ (Table 2) are much smaller than the symbols used to plot the data.

tionate ^{26}Mg from ^{24}Mg by several per mil in such a way that the cold end becomes isotopically heavy. In Section 4, we show that this is indeed the case.

In an effort to minimize the effects of thermal diffusion on the determination of the kinetic isotope fractionation of magnesium by chemical diffusion between basalt and rhyolite, we ran a new diffusion couple, RBX, that was only about half as long as RB11 (~ 5 mm rather than ~ 10 mm) taking special care to center it in the region of uniform temperature of the piston cylinder assembly. Fig. 5 shows the MgO profile and magnesium isotopic data along with calculated model curves. The magnesium isotopic data no longer show a significant gradient in the basalt part of the couple and the calculated fit to the isotopically light magnesium that diffused into the rhyolite is now much improved over that for RB11. The magnesium isotopic data are fit using a kinetic fractionation factor $\beta = 0.05$ in Eq. (2). This value of β is similar to what we found earlier for calcium both in isochemical experiments (Richter et al., 1999) and in rhyolite–basalt diffusion experiments (Richter et al., 2003).

4. THERMAL DIFFUSION

Certain aspects of the elemental profiles measured in diffusion couple RB11 indicated that the experiment had been affected by a temperature difference across the couple. Of particular interest is whether a temperature difference producing a change in magnesium of about 1 wt% can also fractionate the magnesium isotopes by several per mil per atomic mass unit. To explore this possibility we ran a series of piston cylinder experiments with the same assembly as

used for the rhyolite–basalt couples but with the starting material now being entirely SUNY MORB. The basalt sample was placed in the assembly in such a way that the temperature difference across the sample would be about 100–200 °C. The first such experiment, SRT3, was run for 20 h. Later experiments were run for 65 h (SRT8) and 100 h (SRT4). The temperatures above and below the molten basalt in the piston cylinder assembly were determined by juxtaposing MgO and Al_2O_3 at selected point above and below the sample and then using the thickness of the spinel layer produced to determine the local temperature. Fig. 6 shows the temperature profiles in the basalt of the three thermal diffusion experiments.

Major element profiles together with the magnesium isotopic composition in selected points from experiment SRT3 are shown in Fig. 7. The elemental profiles are typical of thermal diffusion (see, for example, the earlier work by Lesher and Walker, 1986). The degree of magnesium isotopic fractionation is surprisingly large with the heavy isotopes enriched towards the cold end. Experiment SRT3 was run for 20 h, which is almost certainly not long enough to display the full fractionations associated with the imposed temperature change. It was run for this length of time to make it comparable to the 15 h run time of the rhyolite–basalt diffusion couple RB11 in order to determine whether a temperature gradient could have produced a significant isotopic fractionation in the basalt side of RB11 in that amount of time. The results make it almost certain that the “anomalous” isotopic fractionations that we observed in the basalt side of RB11 and earlier in RB2 (Richter et al., 2003) are due to thermal diffusion. That similar isotopic fractionations were not seen in the rhyolite–basalt dif-

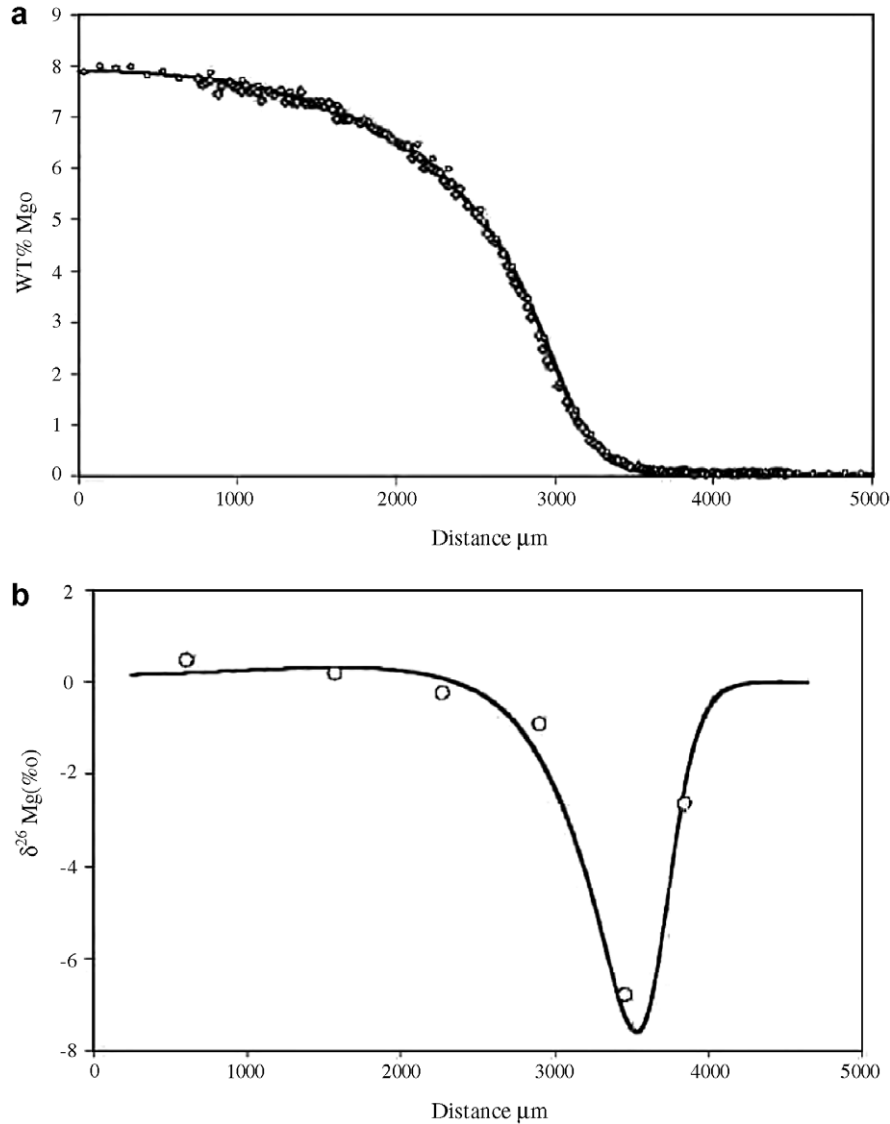


Fig. 5. Magnesium data from rhyolite–basalt diffusion couple RBX together with calculated diffusion profiles for both the wt% MgO and the associated magnesium isotopic fractionation. The diffusion profiles of the other major oxides are like those shown in the left half (5000–10,000 μm) of Fig. 3. The 2σ error bars for $\delta^{26}\text{Mg}$ (Table 2) are much smaller than the symbols used to plot the data. This diffusion couple was intentionally made smaller than RB11 (5 mm vs. 10 mm) in order to minimize the temperature difference from one end to the other of the couple. The calculated profiles use the same dependence of the diffusivities as in Fig. 4 and the fit to the data is now much better than was the case for RB11.

fusion couples RBX and RB3 (in Richter et al., 2003) is explained by there having been significantly less temperature difference across those particular experiments compared to RB11 and RB2.

SRT3 shows that a temperature gradient sufficient to drive about 1 wt% of the MgO component to the cold end of a molten basalt sample can also fractionate magnesium isotopes by many per mil. The 20-h run time of experiment SRT3 was almost certainly too short for the system to have fully equilibrated. The degree to which a thermal diffusion experiment of size L approaches the final steady state as a function of time, t , can be estimated by the factor $1 - e^{-t/\theta}$, where $\theta = L^2/D\pi^2$ (Tyrell, 1961, p. 199). D is an effective binary diffusion coefficient, which we take to be

$7 \times 10^{-7} \text{ cm}^2/\text{s}$ at the average temperature of about 1480 $^\circ\text{C}$ in our experiments (for D in SUNY MORB basalt see Richter et al., 2003). For $L = 8 \text{ mm}$, we get $\theta = 26 \text{ h}$, which suggests that experiment SRT3 had evolved to 54% of the final steady state. Experiment SRT4 was run for 100 h (estimated to be 98% of steady state) to check whether the isotopic fractionations would dissipate as the system approached a steady state. The clear answer is that the isotopic fractionations associated with thermal diffusion persist. Fig. 8 shows the elemental and isotopic fractionation in SRT4 associated with temperature. Experiment SRT8 was run for 63.8 h (92% of steady state) with a smaller temperature difference across the molten basalt (see Fig. 6) to determine how the magnitude of the isotopic frac-

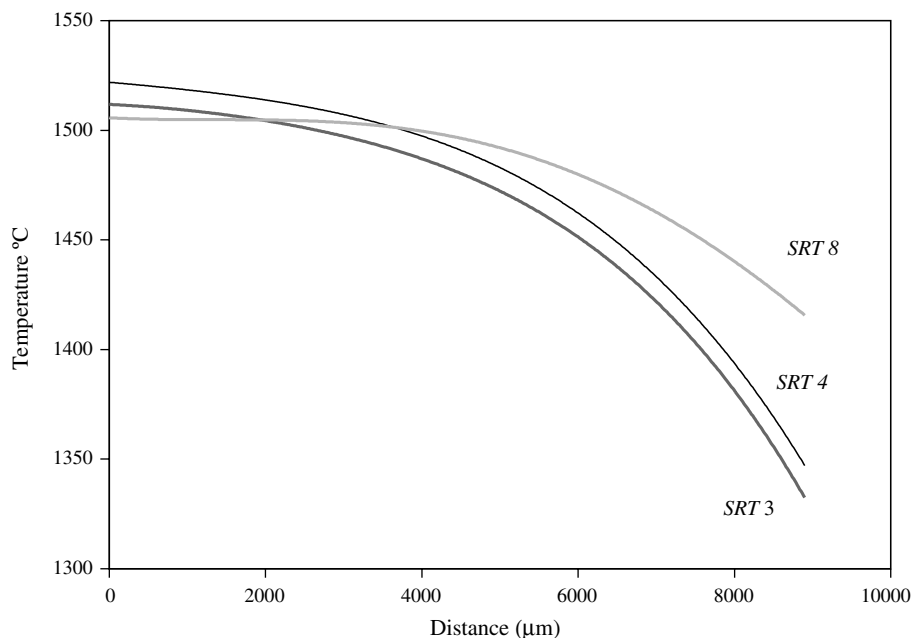


Fig. 6. Temperature estimates in the molten basalt of the three thermal diffusion experiments discussed in the text. The temperature estimates are based on interpolating temperature profiles using data above and below the molten basalt sample as illustrated in Fig. 2.

tionation is related to the temperature difference. Fig. 9 shows that for experiments SRT4 and SRT8 both the elemental and isotopic fractionations in the basalt are to a good approximation linear functions of the temperature and that the slope of the temperature dependence is effectively the same despite differences in run duration and total temperature change across the two samples. The fact that we found no significant difference between the slope of the elemental and isotopic fractionations as a function of temperature in experiments SRT4 and SRT8 suggests that the results had become effectively independent of time and thus can be used to provide a reasonable estimate of the steady state condition.

5. DISCUSSION

We were surprised to find that even relatively small temperature differences across a rhyolite–basalt diffusion couple could give rise to large isotopic fractionations that make quantifying the kinetic isotopic fractionations due to the chemical diffusion problematic. Our attempt to fit the magnesium isotopic data from experiment RB11 (Fig. 4) illustrates the problem. We attempted to minimize the effects of temperature gradients in a second rhyolite–basalt diffusion couple (RBX) by making it smaller (about 5 mm in its largest dimension) and being careful to place it in that part of the piston cylinder assembly that has the most uniform temperature. The elemental profiles measured in RBX showed no evidence of thermal diffusion effects, and we were reasonably successful in fitting the measured elemental and magnesium isotopic data with model calculations (Fig. 5). The kinetic fractionation of magnesium diffusing from the basalt into the rhyolite side of the diffusion couple was fit using $\beta = 0.05$ in our parameteriza-

tion Eq. (2) for the relative mobility of the magnesium isotopes. This value of β for magnesium isotopes is similar to that found earlier by Richter et al. (2003) for calcium ($\beta \approx 0.075$) but much smaller than what they found for lithium ($\beta \approx 0.215$). The significance for natural systems of the kinetic isotope fractionations of magnesium we have demonstrated in laboratory has not yet been established. However, we are encouraged in terms of potential applications of diffusive isotope fractionations to natural situations by the recent report by Teng et al. (2006) of very large ($\sim 30\%$) lithium isotopic fractionations associated with the diffusion of lithium from the Tin Mountain pegmatite into a surrounding amphibolite.

The kinetic isotopic fractionation we measured for magnesium diffusing from basalt into rhyolite is pretty much as predicted in Richter et al. (2003). The result that was unexpected was the extraordinarily large isotopic fractionation of magnesium associated with thermal diffusion in molten basalt. Kyser et al. (1998) had already shown that a large temperature gradient of about 200 °C over 4 mm could fractionate oxygen isotopes by up to 2.5‰/amu, but this is considerably smaller than 4‰/amu for the magnesium isotopic fractionations that we found for a temperature gradient of only 100 °C over about 8 mm. One measure of how extraordinary large the thermal fractionations of magnesium isotopes are is to compare them to what has been found in the case of gases at low temperature (≤ 0 °C). A reasonable expectation would have been that isotopic fractionations in gases should be much larger than in condensed systems, which is certainly the case for isotopic fractionation by chemical diffusion, and at least for equilibrium fractionations, the lower the temperature the larger the effect. Contrary to these expectations, we found, for example, that the thermal fractionation of magnesium in a silicate li-

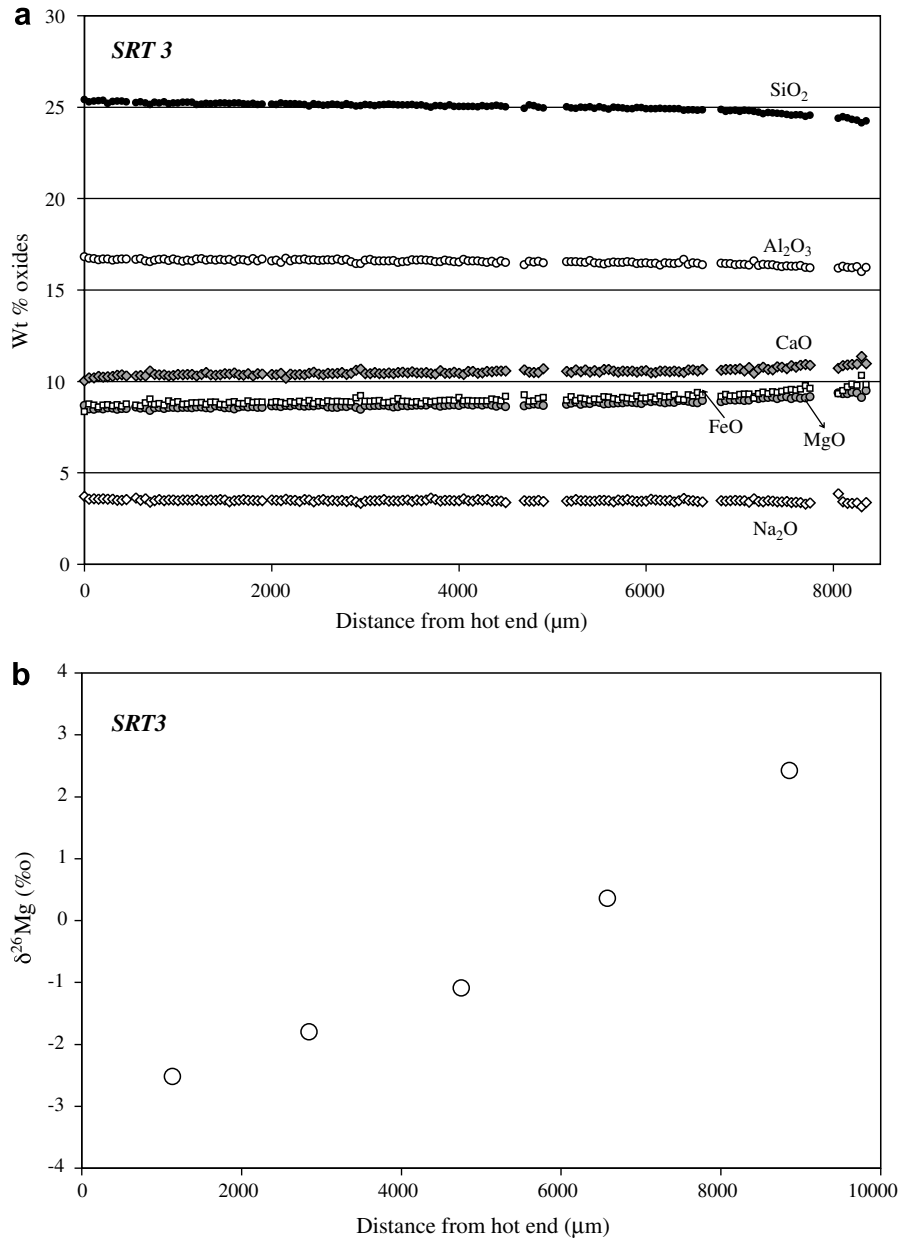


Fig. 7. (a) Composition profiles in wt% of the major oxides of basalt in quenched glass from the 20-h thermal diffusion experiment SRT3. The actual wt% of SiO_2 is twice the amount shown. (b) Magnesium isotopic fractionation in per mil at various distances from the hotter end of the basalt sample. The 2σ error bars for $\delta^{26}\text{Mg}$ are much smaller than the symbols.

liquid is much larger than that of nitrogen in air. Severinghaus et al. (2001) use a parameter they call the thermal diffusion sensitivity Ω to measure the effectiveness of thermal diffusion in separating isotopes. Ω is defined as the isotopic fractionation per atomic mass unit per degree centigrade temperature difference (i.e., $\text{‰}/^\circ\text{C}/\text{amu}$). For $^{29}\text{N}_2/^{28}\text{N}_2$, either alone or in air, $\Omega \approx 1.5 \times 10^{-2}\text{‰}/^\circ\text{C}$ for temperatures in the range -60°C to 0°C (Grachev and Severinghaus, 2003). The slope of the relationship between magnesium isotope fractionation and temperature shown in Fig. 9b corresponds to $\Omega \approx 3.6 \times 10^{-2}\text{‰}/^\circ\text{C}/\text{amu}$, which is more than twice as large as the thermal sensitivity factor for such a relatively inert gas as nitrogen. That thermal diffusion in a

liquid such as basalt should be so much more effective at fractionating isotopes than thermal separations in a gas phase is quite remarkable.

Having found large isotopic fractionations of magnesium by thermal diffusion in molten basalt, we thought it might prove to be a useful way of determining the relative mobility of isotopes. Our usual approach for measuring the relative mobility of isotopes has been to use diffusion couples such as those discussed in Section 3. In the case of diffusion couples the kinetic fractionations due to the relative mobility of the isotopes is largest in those parts of the couple with very low abundance of the parent element, which makes it quite difficult to obtain high-precision data

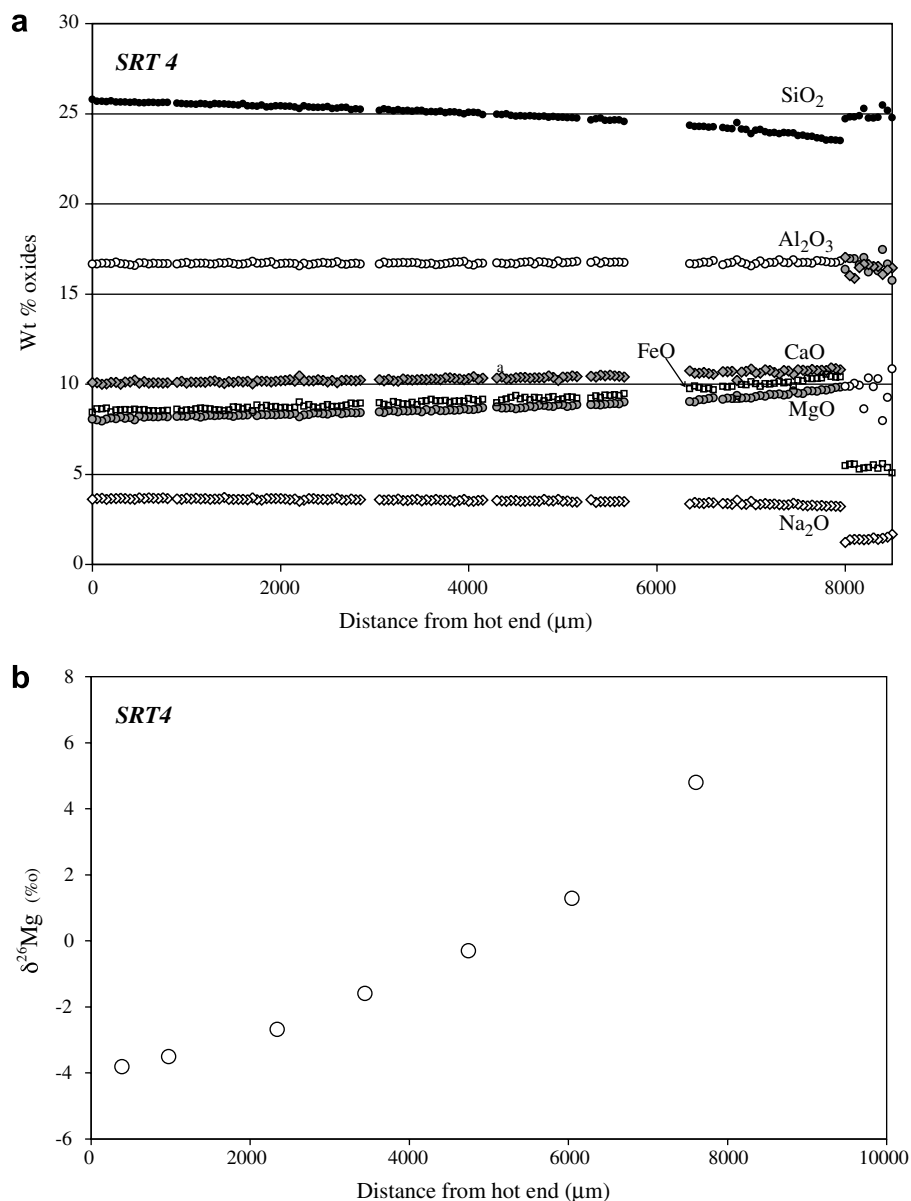


Fig. 8. Same as Fig. 7 but now for the 100-h thermal diffusion experiment SRT4. The effect of olivine crystallization can be seen in the scattered wt% of the oxides in that part of the sample beyond 8000 μm. Given that Teng et al. (2007) have shown that olivine crystallizing from a basalt melt does not fractionate magnesium isotopes, we do not believe that the magnesium isotopic fractionations shown in part (b) have been affected by the fractional crystallization of olivine in the coldest parts of the sample. The 2σ error bars for $\delta^{26}\text{Mg}$ (Table 2) are much smaller than the symbols used to plot the data.

for determining the kinetic fractionation parameter β in Eq. (2). There is also the problem that there are, by design, large compositional gradients in a traditional chemical diffusion experiment used to determine isotope fractionations and thus the results cannot be said to be a property of any specific composition. The hope was that thermal diffusion might provide a more effective way of determining the relative mobility of isotopes. A thermal diffusion experiment has the distinct advantage that the system would be much less variable in composition than the usual chemical diffusion experiment and that the isotopic measurements would be made in places where the abundance of the parent ele-

ment was not much changed from the original bulk composition of the starting material.

Our idea of how one might extract isotope mobility from thermal diffusion experiments is based on a simplified version of the representation of mass fluxes in liquids subjected to a thermal gradient given in Tyrell (1961). A commonly used flux equation, even though it is strictly valid only for a binary system (Eq. (3.25) in Tyrell, 1961; see also Eq. (227) in deGroot and Mazur, 1984; CH. XI §7), is of the form

$$J_i = -D_i\rho(dw_i/dx + \sigma_i w_i w_j dT/dx) \quad (3)$$

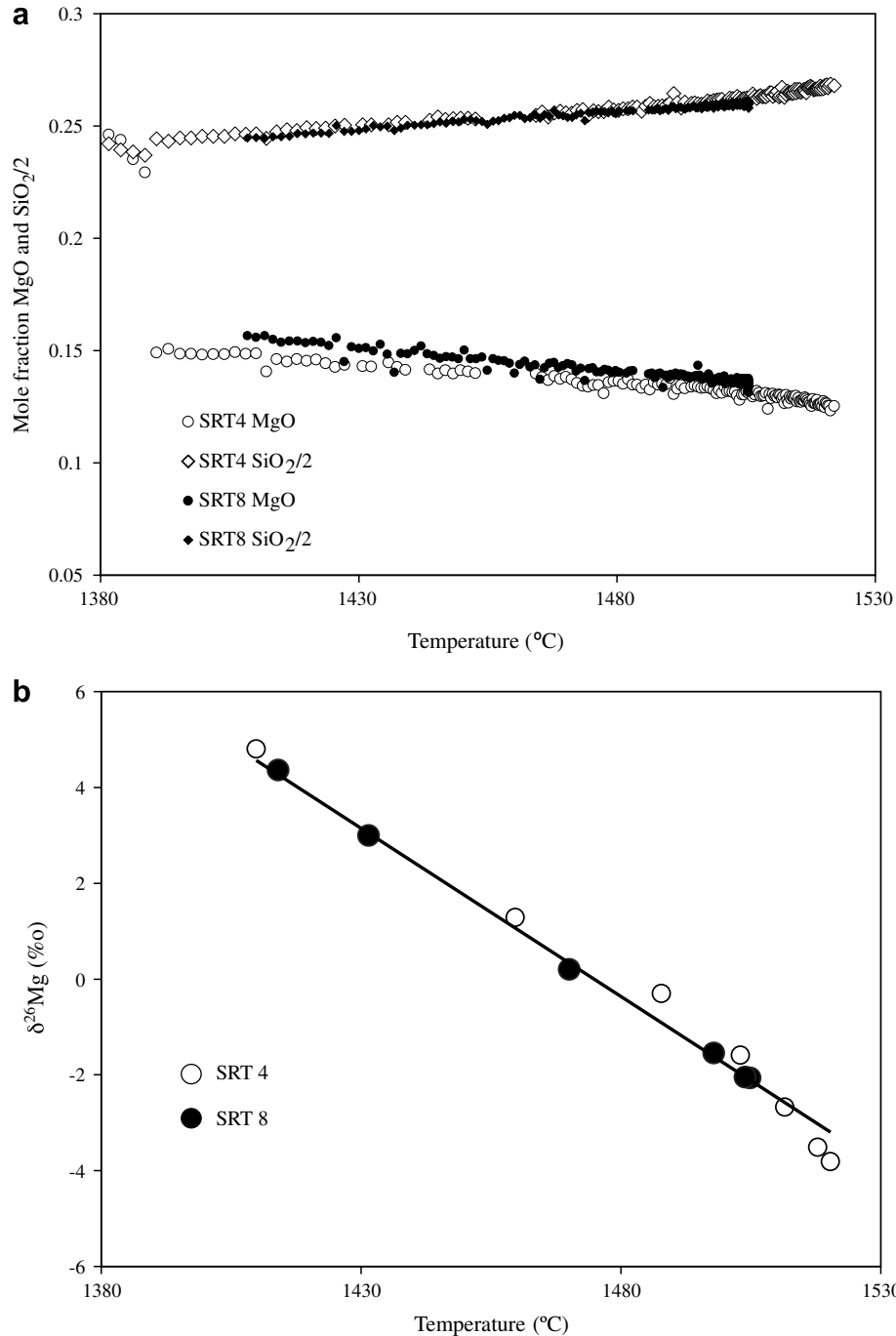


Fig. 9. (a) Correlation of the SiO₂ and MgO mole fractions in the melt with temperature for thermal diffusion experiments SRT4 and SRT8. The slope of the correlations of mole fraction with temperature correspond to Soret coefficients $\sigma_{\text{MgO}} = 1.63 \times 10^{-3}$ for SRT4 and $\sigma_{\text{MgO}} = 1.77 \times 10^{-3}$ for SRT8 (see text for the definition of the Soret coefficient). The small offset of the MgO mole fractions between SRT4 and SRT8 are most likely due to a small amount of olivine that crystallized in the coldest parts of sample SRT4. (b) Correlation of the magnesium isotopic composition with temperature in thermal diffusion experiments SRT4 and SRT8. The slope of the best fitting line through combined data corresponds to a thermal diffusion sensitivity factor $\Omega = 3.6 \times 10^{-2} \text{‰/}^\circ\text{C}$ per atomic mass unit.

where D_i is the effective binary diffusion coefficient of component i in the mixture of i and j , ρ is the density of the mixture, w_i and w_j are the mass fractions of i and j , and σ_i is the Soret coefficient. Once the system achieves a steady state (i.e., $J_i = 0$), the Soret coefficient can be evaluated using experimental data in the expression

$$\sigma_i = -\frac{1}{w_i w_j} \frac{dw_i}{dT} \quad (4)$$

Leshner and Walker (1986) calculated Soret coefficients for various components of silicate liquids using a slightly modified pseudo-binary equivalent of Eq. (4) with the w_i becoming mole fractions such that

$$\sigma_i = -\frac{1}{(1 - \bar{w}_i)\bar{w}_i} dw_i/dT \quad (5)$$

where \bar{w}_i is the mole fraction of component i in the bulk composition. We can use the Soret coefficient as defined by Eq. (5) to compare our results to those given by Lesher and Walker (1986) for their thermal diffusion experiments with a slightly more silica-rich mid-ocean ridge basalt than the one we used here. We get $\sigma_{\text{MgO}} = 1.77 \times 10^{-3}$ and $\sigma_{\text{SiO}_2} = -1.29 \times 10^{-3}$ for experiment SRT8 and $\sigma_{\text{MgO}} = 1.63 \times 10^{-3}$ and $\sigma_{\text{SiO}_2} = -1.51 \times 10^{-3}$ for experiment SRT4 compared to $\sigma_{\text{MgO}} = 2.70 \times 10^{-3}$ and $\sigma_{\text{SiO}_2} = -2.29 \times 10^{-3}$ for the longest duration (264 h) basalt experiment reported by Lesher and Walker (1986). The differences between the Soret coefficients derived from our experiments and those of Lesher and Walker (1986) may reflect the fact that we used different basalt compositions and/or that they had more fully achieved a steady state given the longer duration of their experiment. The differences might also be due to the fact that the Lesher and Walker (1986) basalt experiments involved a much less uniform system than ours both in terms of the large change in composition in their experiments (e.g., SiO₂ changing by ~12 wt%, MgO changing by ~4 wt%) and a much larger temperature difference ($\Delta T = 300$ °C) than that in our experiments.

Our attempt to determine the relative mobilities of magnesium isotopes from thermal diffusion experiments is based on using Eq. (3) to write a steady state expression for the magnitude of the change in total magnesium due to the thermal gradient and assume similar expressions for the individual isotopes. We can rewrite Eq. (3) using Eq. (5) as

$$J_i = -\rho(D_i dw_i/dx + D_T^i \bar{w}_i(1 - \bar{w}_i)dT/dx) \quad (6)$$

where we have introduced a thermal diffusion coefficient, D_T^i , for species i such that $\sigma_i = D_T^i/D_i$. The steady state ($J_i = 0$) expressions for total magnesium and for isotopes i are

$$dw_{\text{Mg}}/dT = -\hat{D}_T^{\text{Mg}}/D_{\text{Mg}} \quad (7)$$

where $\hat{D}_T^{\text{Mg}} = \bar{w}_{\text{Mg}}(1 - \bar{w}_{\text{Mg}})D_T^{\text{Mg}}$ is a modified thermal diffusion coefficient for magnesium that can be evaluated from the experimental data of the slope of w_{Mg} versus T .

$$dw_i/dT = -X_i(\hat{D}_T^i/D_i) \quad i = {}^{24}\text{Mg}, {}^{25}\text{Mg}, \text{ or } {}^{26}\text{Mg} \quad (8)$$

where X_i is the atom fraction of magnesium isotope i in the total magnesium (i.e., $\sum X_i = 1$), D_i is the chemical diffusion coefficient of isotope i , and $\hat{D}_T^i = \bar{w}_{\text{Mg}}(1 - \bar{w}_{\text{Mg}})D_T^i$ is the modified thermal diffusion coefficient of isotope i . In writing Eq. (8) we have assumed that the flux of the individual isotopes driven by the thermal gradient is proportional to the fraction of that isotope relative to the total magnesium. We can allow for a mass dependence of the thermally driven flux by letting it appear as a mass dependence of \hat{D}_T^i . We further assume that

$$\hat{D}_T^{24}/D_{24} = \hat{D}_T^{\text{Mg}}/D_{\text{Mg}} \quad (9)$$

because the ratio of the diffusion coefficients of total Mg is the best estimate we have for this ratio in the case of ²⁴Mg, which corresponds to about 80% of the total magnesium.

This choice is not critical because for present purposes what really matters is the mass dependence of this ratio, not its exact magnitude. We allow for the mass dependence of the diffusion coefficients by the relationship

$$\hat{D}_T^{26}/D_{26} = (\hat{D}_T^{24}/D_{24})(26/24)^{\beta+\beta_T} \quad (10)$$

where the parameter β comes from the mass dependence of the D_i in Eq. (2) and the mass dependence of the thermal diffusion coefficient is assumed to be of the form $\hat{D}_T^{26}/D_{26} = (26/24)^{\beta_T}$. Combining Eqs. (8)–(10) gives

$$dw_{24}/dT = -X_{24}(\hat{D}_T^{\text{Mg}}/D_{\text{Mg}}) \quad (11)$$

$$dw_{26}/dT = -X_{26}(\hat{D}_T^{\text{Mg}}/D_{\text{Mg}})(26/24)^{\beta+\beta_T} \quad (12)$$

The atom fraction X_i can be expressed in term of w_i by $X_i = w_i/w_{\text{Mg}}$. Eqs. (11) and (12) can then be written as

$$d \ln w_{24}/dT = -(\hat{D}_T^{\text{Mg}}/D_{\text{Mg}})/w_{\text{Mg}} \quad (13)$$

$$d \ln w_{26}/dT = -(\hat{D}_T^{\text{Mg}}/D_{\text{Mg}})(26/24)^{\beta+\beta_T}/w_{\text{Mg}} \quad (14)$$

Ignoring a small (and for present purposes negligible) difference between w_{Mg} and \bar{w}_{Mg} , we can integrate Eqs. (13) and (14) from the cold end ($T = T_c$) to the hot end ($T = T_h$) and then subtract the second integral from the first one. A minor manipulation of the resulting equation yields

$$\ln \left(\frac{(w_{26}/w_{24})_{\text{cold}}}{(w_{26}/w_{24})_{\text{hot}}} \right) = \left[(\hat{D}_T^{\text{Mg}}/D_{\text{Mg}})\Delta T/\bar{w}_{\text{Mg}} \right] \left[(26/24)^{\beta+\beta_T} - 1 \right] \quad (15)$$

All quantities other than $\beta + \beta_T$ in Eq. (15) can be obtained from the experimental data. $\left(\frac{(w_{26}/w_{24})_{\text{cold}}}{(w_{26}/w_{24})_{\text{hot}}} \right)$ is the ratio of ²⁶Mg/²⁴Mg between the cold and the hot end of the sample (change in $\delta^{26}\text{Mg}/1000 + 1$) for a temperature difference $\Delta T = T_h - T_c$. The slope of the isotopic data versus temperature in Fig. 9b provides an estimate of $\left(\frac{(w_{26}/w_{24})_{\text{cold}}}{(w_{26}/w_{24})_{\text{hot}}} \right) = 1.007$ for $\Delta T = 100$ °C. $(\hat{D}_T^{\text{Mg}}/D_{\text{Mg}})/\bar{w}_{\text{Mg}} = (1 - \bar{w}_{\text{Mg}})\sigma_{\text{Mg}}$. $1 - \bar{w}_{\text{Mg}} = 0.86$ and the average Soret coefficient from experiments SRT4 and SRT8 is $\sigma_{\text{Mg}} = 1.7 \times 10^{-3}$. These quantities result in an estimate $\beta + \beta_T \approx 0.6$. If we accept that rhyolite–basalt experiment RBX provides a reasonable estimate of the mass dependence of the chemical diffusion coefficient for magnesium (i.e., $\beta \approx 0.05$), then $\beta_T \approx 0.55$ and the thermal diffusion coefficient for magnesium depends on mass by an amount corresponding to $D_T^{\text{Mg}26}/D_T^{\text{Mg}24} \approx (26/24)^{0.55}$. The obvious implication is that the thermally driven flux is far more mass-dependent and thus far more effective at fractionating isotopes than the flux due to concentration gradients. Furthermore, the thermal diffusion coefficient increases with the mass of the isotope whereas the reverse is true for the chemical diffusion coefficient. The fact β_T is not negligibly small compared to β precludes using thermal isotope fractionations (i.e., Eq. (15)) to determine the kinetic isotope fractionation factor β for chemical diffusion.

There are a number of potential applications of the large isotopic fractionation that we found associated with thermal gradients in molten silicates. Given that a temperature difference of only about 100 °C in a basalt liquid can produce about a 1% fractionation of ²⁶Mg from ²⁴Mg it would seem that by using larger temperature differences and

exploring the effect of other compositions a very effective condensed phase isotope separation method could be developed. In terms of implications and applications to experimental petrology, it is now quite clear that in order to measure kinetic isotope fractionations in molten silicates great care will have to be taken to insure that the system is effectively isothermal. The thermal isotope fractionation could also be used to map the temperature distribution in samples recovered from high-pressure experiments run in piston cylinder apparatus and in large-volume multi-anvil presses. If necessary the samples could be analyzed for isotope differences using a multi-collector ion probe which we have shown (Richter et al., 2007) is capable of 0.1‰ precision in measuring $\delta^{26}\text{Mg}$ on 10 μm spots. Given the correlation of $\delta^{26}\text{Mg}$ and temperature shown in Fig. 9, a precision of 0.1‰ in $\delta^{26}\text{Mg}$ translates into a precision for measuring temperature of about 2 °C.

When thinking about the relevance of elemental and isotopic fractionations due to thermal gradients to the properties of igneous rocks one has to contend with Bowen's (1921) assessment that these will not be important other than in very special situations because of the short time scale over which the thermal gradients dissipate compared to the much longer time it would take for the chemical fractionations to develop. Bowen was a powerful advocate of fractional crystallization as the key mechanism for developing the range of composition of the major igneous rocks. Given Bowen's strong influence on experimental petrology, it took quite a long time before there would be much interest in exploring or invoking other processes that might give rise to chemical fractionations in molten silicate systems. There was a short-lived revival of interest in alternative igneous fractionation mechanisms due in part to recurring observations of chemical trends in igneous systems that could not be easily explained in terms of partial melting and crystal fractionation (see, for example, Hildreth, 1979, 1981). An added stimulus for this renewal of interest in alternative fractionation mechanisms in molten silicate systems was a series of experimental studies of Soret fractionation by Dave Walker and collaborators (Walker et al., 1981; Walker and DeLong, 1982). These experiments demonstrated that thermal diffusion could produce large differences in silicate liquid composition comparable in magnitude to that arising from crystal fractionation. The fact that the trends in composition space produced by crystal fractionation versus thermal fractionation were in many cases distinct was used to interpret "anomalous" trends in the Bishop magma (Hildreth, 1979, 1981), lunar rocks (Walker et al., 1981), and mid-ocean ridge magmas (Walker and DeLong, 1982). However, once more detailed experiments were carried out (Leshner and Walker, 1986) and the results compared to fractionations observed in natural systems it became increasingly apparent that liquid-state fractionations due to Soret diffusion are not a plausible mechanism for the distinctive geochemical features of the Bishop Tuff (see Leshner and Walker, 1991 for a more extended discussion of role of thermal diffusion in petrology).

Our demonstration that thermal fractionations of basalt chemistry will be marked by large isotopic fractionations of an element such as magnesium that is otherwise of quite

uniform isotopic composition in nature (see the Teng et al., 2007 demonstration that crystal fractionation from a basalt does not produce measurable magnesium isotopic effects) can provide a quantitative test of whether an observed chemical trend in an igneous system can be attributed to thermal fractionation. We agree with the view that thermal fractionations are not important in effecting large-scale chemical fractionations of natural igneous systems. Had thermal fractionations been important on a large scale, one should find large differences in the magnesium isotopic composition of igneous rocks, but no such differences have been found. It remains, however, quite plausible that Soret fractionations will arise in certain local settings such as thermal boundary layers where temperature gradients can be maintained for long periods of time by the advection of heat. The distinctive isotopic fractionations associated with Soret processes in molten silicate systems can provide a diagnostic test of whether thermal gradients persisted for a sufficient length of time in a natural setting to effect chemical fractionations and to distinguish these from other processes such as mixing or melt contamination by assimilation of the host rocks.

ACKNOWLEDGMENTS

The reviewers of the original manuscript, and especially Charles Leshner, made a number of important comments and suggestions that resulted in a much improved final manuscript. The research reported in this paper was supported by grant from the Department of Energy to Frank Richter (DE-FG02-01ER15254, A005) and National Science Foundation grant to Bruce Watson (EAR-0337481).

REFERENCES

- Bowen N. L. (1921) Diffusion in silicate melts. *J. Geol.* **29**, 295–317.
- deGroot S. R. and Mazur P. (1984) *Non-Equilibrium Thermodynamics*. Dover Publications, New York, 510 pp.
- Galy A., Belshaw N. S., Halicz L. and O'Nions R. K. (2001) High-precision measurement of magnesium isotopes by multiple-collector inductively coupled plasma mass spectrometry. *Int. J. Mass Spectrom.* **208**, 89–98.
- Galy A., Yoffe O., Janney P. E., Williams R. W., Cloquet C., Alard O., Halicz L., Wadhwa M., Hutcheon I. D., Ramon E. and Carignan J. (2003) Magnesium isotope heterogeneity of the isotopic standard SRM980 and new reference materials for magnesium-isotope-ratio measurements. *J. Anal. At. Spectrom.* **18**, 1352–1356.
- Grachev A. M. and Severinghaus J. P. (2003) Laboratory determination of thermal diffusion constants for $^{29}\text{N}_2/^{28}\text{N}_2$ in air at temperatures from -60 to 0°C for reconstruction of the magnitudes of abrupt climate changes using the ice core fossil-air paleothermometer. *Geochim. Cosmochim. Acta* **67**, 345–360.
- Hildreth W. (1979) The Bishop Tuff: evidence for the origin of compositional zonation in silicic magma chambers. *Geol. Soc. Am. Spec. Pap.* **180**, 43–75.
- Hildreth W. (1981) Gradients in silicic magma chambers: implications for lithospheric magmatism. *J. Geophys. Res.* **86**, 10153–10192.
- Kyser T. K., Leshner C. E. and Walker D. (1998) The effects of liquid immiscibility and thermal diffusion on oxygen isotopes in silicate liquids. *Contrib. Mineral. Petrol.* **133**, 373–381.
- Leshner C. E. and Walker D. (1986) Solution properties of silicate liquids from thermal diffusion experiments. *Geochim. Cosmochim. Acta* **50**, 1397–1411.

- Leshner C. E. and Walker D. (1991) Thermal diffusion in petrology. In *Diffusion, Atomic Ordering, and Mass Transport*, vol. 8 (ed. J. Ganguly). Advances in Physical Geochemistry. Springer-Verlag, New York, pp. 396–451.
- Richter F. M., Liang Y. and Davis A. M. (1999) Isotope fractionation by diffusion in molten oxides. *Geochim. Cosmochim. Acta* **63**, 2853–2861.
- Richter F. M., Davis A. M., DePaolo D. J. and Watson E. B. (2003) Isotope fractionation by chemical diffusion between molten basalt and rhyolite. *Geochim. Cosmochim. Acta* **67**, 3905–3923.
- Richter F. M., Kita N. T., Mendybaev R. A., Davis A. M. and Valley, J. W. (2007) High-precision Mg isotopic composition of Type B1 and B2 CAI melilite. *Lunar Planet. Sci.* **XXXVIII**, Abstract # 2303.
- Severinghaus J. P., Grachev A. and Battle M. (2001). Thermal fractionation of air in polar firn by seasonal temperature gradients. *Geochim. Geophys. Geosys.* **2**, #2000GC000146.
- Teng F.-Z., Wadhwa M. and Helz R. T. (2007) Investigation of magnesium isotope fractionation during basalt differentiation: implications for a chondritic composition of the terrestrial mantle. *Earth Planet. Sci. Lett.* **261**, 84–92.
- Teng F.-Z., McDonough W. F., Rudnick R. L. and Walker R. J. (2006) Diffusion-driven extreme lithium isotopic fractionation in country rocks of the Tin Mountain pegmatite. *Earth Planet. Sci. Lett.* **243**, 701–710.
- Tyrell H. J. V. (1961) *Diffusion and Heat in Liquids*. Butterworths, London, 329 pp.
- Walker D., Leshner C. E. and Hays J. F. (1981) Soret separation of a lunar liquid. *Proc. Lunar Planet. Sci.* **12B**, 991–999.
- Walker D. and DeLong S. E. (1982) Soret separation of mid-ocean ridge basalt magma. *Contrib. Mineral. Petrol.* **79**, 231–240.
- Watson E. B., Wark D. A., Price J. D. and Van Orman J. A. (2002) Mapping the thermal structure of solid-media pressure assemblies. *Contrib. Mineral. Petrol.* **142**, 640–652.

Associate editor: F.J. Reyerson